Fluctuations and correlations from NA61/SHINE

Marek Gazdzicki[*]

Goethe-Univeristy Frankfurt am Main,
Jan Kochanowski University Kielce
E-mail: marek@cern.ch

for the NA61/SHINE Collaboration

Basic ideas, methods and results related to the NA61/SHINE study of event-by-event fluctuations in high energy nuclear collisions are briefly reviewed.

---

[*]Speaker.

1. Introduction

Study of event-by-event fluctuations is the focus of the NA61/SHINE programme on strong interactions. Initially the study was motivated by the possibility to discover the critical point of strongly interacting matter and a need to understand how the onset of deconfinement influences event-by-event fluctuations [1]. Recently, results on fluctuations together with data on mean hadron multiplicities allowed to uncover the onset of fireball [1] - the rapid change of hadron production properties that start when moving from Be+Be to Ar+Sc collisions [2].

Fluctuations in high energy collisions are significantly influenced by fluctuations in the amount of matter (*volume*) and energy involved in a collision, as well as global and local conservation laws. In the search for the critical point and the study of the onset of deconfinement these are unwanted effects [3]. However, the onset of fireball was discovered thanks to the sensitivity of fluctuations to the conservation laws [2]. Moreover, the dynamics of the early stage of the collision can be studied exploiting *volume* fluctuations [4].

In this contribution *volume* fluctuations are treated as unwanted effect and methods to remove their influence are presented in Secs. 2 and 4. The conservation laws are in Sec. 3 treated as a tool to uncover the onset of fireball and in Sec. 4 as to-be-minimized bias in the search for the critical point.

2. Removing *volume* fluctuations

It is probably the simplest to introduce fluctuations of the amount of matter involved in a collision and their impact on fluctuations of produced particles using as an example the Wounded Nucleon Model [5]. The model was proposed in 1976 as a late child of the S-matrix period [6]. It assumes that particle production in nucleon-nucleon and nucleus-nucleus collisions is an incoherent superposition of particle production from wounded nucleons (nucleons which interacted inelastically and whose number is calculated using straight line trajectories of nucleons). Properties of wounded nucleons are independent of the size of colliding nuclei, e.g. they are the same in p+p and Pb+Pb collisions at the same collision energy per nucleon. These assumptions are graphically illustrated in Fig. 1.

Let us consider multiplicity (particle number) fluctuations characterized by second moments of multiplicity distributions. Two quantities of relevance are variance, $Var[N] = \langle (N - \langle N \rangle)^2 \rangle$ and scaled variance, $\omega[N] = Var[N]/\langle N \rangle$. Here N and $\langle N \rangle$ stand for multiplicity and its mean value, respectively. Then for any probability distribution $P(W)$, the scaled variance calculated within WNM reads [7]:

$$\omega[N] = \omega[N]_W + \langle N \rangle / \langle W \rangle \cdot \omega[W] \, , \tag{2.1}$$

where $\omega[N]_W$ stands for the scaled variance at any fixed number of wounded nucleons, and $W = W_P + W_T$ for the sum of the number W_P and W_T of projectile and target nucleons. Here the first component of Eq. 2.1 is considered to be the wanted one, whereas the second one is unwanted. Similar relations are valid for Statistical Models of an Ideal Boltzmann gas within the Grand Canonical Ensemble SM(IB-GCE) [7].

---

[1]The name was proposed by Edward Shuryak during the CPOD 2017 workshop in Stony Brook
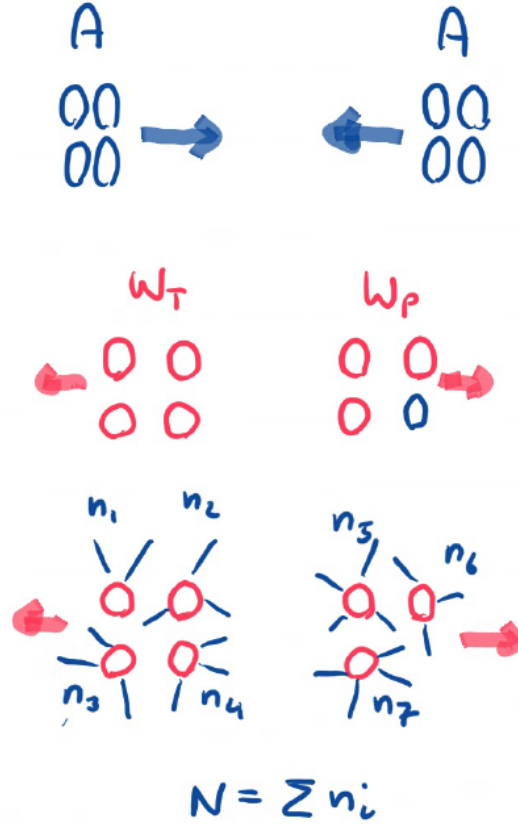
Figure 1: Sketch of particle production in nucleus-nucleus collisions according to the Wounded Nucleon Model. Projectile and target nuclei with nuclear mass number A_P and A_T (here $A = A_P = A_T = 4$) collide. W_T (here $W_T = 4$) target wounded nucleons and W_P (here $W_P = 3$) projectile wounded nucleons produce N particles, where N is given by the sum over all wounded nucleons of particle multiplicities n from single wounded nucleons.

In order to limit the unwanted component NA61/SHINE selects collisions with the smallest energy recorded by the Projectile Spectator Detector - the calorimeter that predominantly measures energy of projectile spectators, see Fig. 2. Multiplicity fluctuations for the selected most violent collisions (collisions with the largest W_P) are only weakly increased by W fluctuations. This is demonstrated in Fig. 3 based on simulations performed with the HSD and UrQMD models [8].

Since even for the most violent collision volume fluctuations cannot be fully eliminated, it is important to further minimise their effect by defining suitable fluctuation measures. It appears that using second and first moments of the distribution of two extensive quantities (their first moments are proportional to *volume*) one can construct fluctuation measures which are, for the WNM and the SM(IB-GCE) models [9, 7, 10], independent of *volume* fluctuations.

In particular, one can construct the strongly intensive scaled variance [7],

$$\Omega[N, E_P] = \omega[N] - (\langle N \cdot E_P \rangle - \langle N \rangle \cdot \langle E_P \rangle)/\langle E_P \rangle \,, \tag{2.2}$$
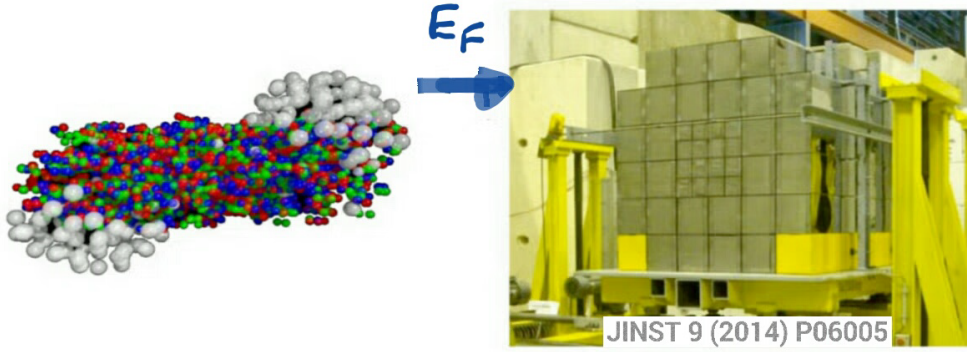
2

Figure 2: Energy E_F recorded in a set of modules of the Projectile Spectator Detector is used to select the most violent nucleus-nucleus collisions. E_F is dominated by the energy of projectile spectators.
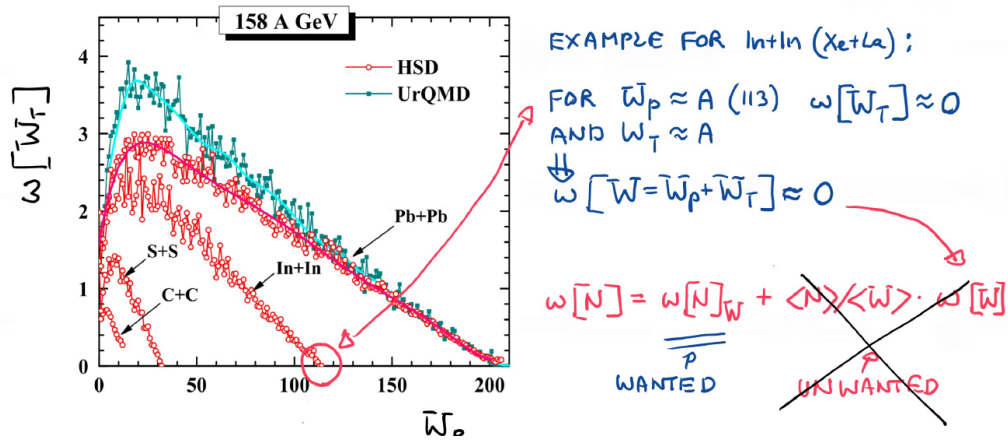

Figure 3: Scaled variance of the dsitribution of the number W_T of wounded target nucleons as a function of the number W_P of wounded projectile nucleons calculated with the HSD and UrQMD models for different nucleus-nucleus collisions.

where $E_P = E_{BEAM} - E_F$. It is easy to show that

$$\Omega[N, E_P] \approx \omega[N]_W = \omega[n] \tag{2.3}$$

under two conditions $\langle N \cdot E_P \rangle_W \approx \langle N \rangle_W \cdot \langle E_P \rangle_W$ and $\langle E_P \rangle_W \sim W$ that are expected to be fulfilled for violent A+A collisions.

The above defined procedures to minimize the effects of *volume* fluctuations were tested using theoretical models and experimental data. An exmaple of the experimental test performed for Be+Be collisions at 75A GeV/c is presented in Fig. 4. The scaled variance ω increases with increasing percentile of violent collisions selected for the analysis using the measured values of E_F. The strongly intensive scaled variance Ω is almost independent of the percentile of selected collisions. The two coincide for the most violent collisions.
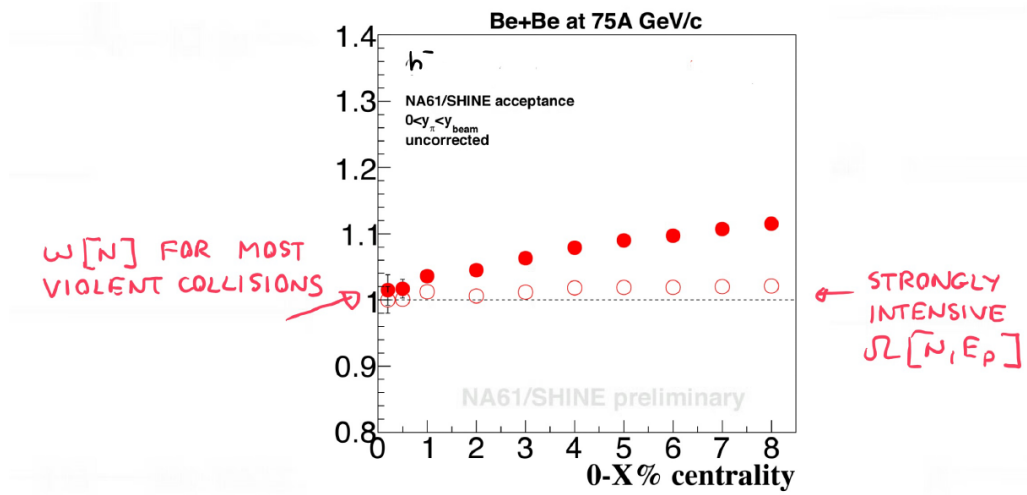
3

Figure 4: Comparison of the scaled variance of the negatively charged hadron multiplicity distribution with the corresponding strongly intensive scaled variance for Be+Be collisions at 75A GeV/c for different selections of violent (central) collisions. For detail see Ref. [11].
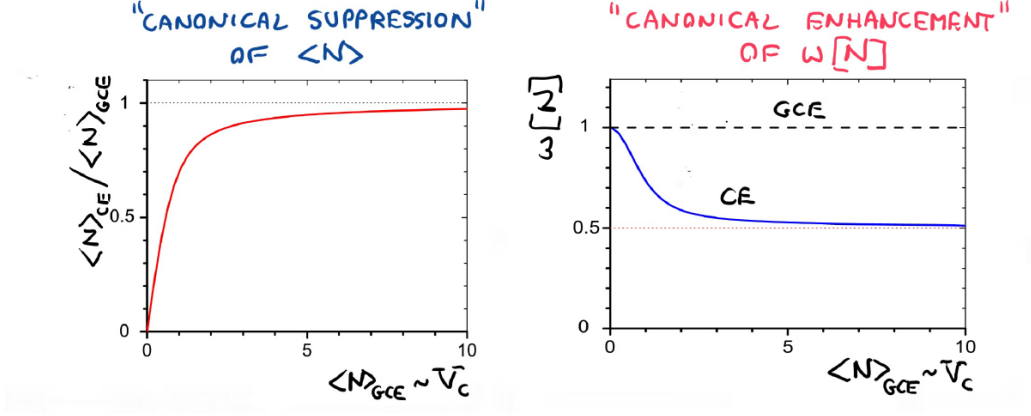
3. Exploiting conservation laws

Figure 5: The ratio of mean multiplicities (*left*) and scaled variance (*right*) calculated for the SM(IB-CE) and SM(IB-GCE) ensembles are plotted as a function of the mean multiplicity for SM(IB-GCE), the latter being proportional to the cluster volume, V_C. The calculations are done for a gas of positively and negatively charged particles with total charge equal to zero.

The most efficient description of bulk properties of hadron production in high energy heavy ion collisions is given by statistical and hydrodynamical models [12]. Thus, here the impact of conservation laws on mean multiplicity and multiplicity fluctuations is discussed with statistical models. For simplicity consider only material conservation laws (conserved charges: Q, B, S, ...). Then the simplest model is a Statistical Model with Ideal Boltzmann Gas using the Canonical Ensemble, SM(IB-CE). In this model correlations between particles are only due to material conservation laws. Their influence on mean multiplicity and scaled variance is presented in Fig. 5, where results for a gas of positively and negatively charged particles contained in a cluster of volume V_C and with total charge equal to zero are shown as a function of mean multiplicity calculated with the SM(IB-GCE). Note that the mean multiplicity in the SM(IB-GCE) is proportional to the cluster volume provided the temperature is independent of V_C. The well know "canonical suppression" of the mean multiplicity [13] and a somewhat less well known "canonical enhancement" of the scaled variance [14] are seen. Note that in the large V_C limit the results for the mean multiplicity obtained with the SM(IB-CE) and SM(IB-GCE) are equal and for the scaled variance they remain different.

In the following the qualitative expectations derived from the SM(IB-CE) will be confronted with experimental data. Figure 6 shows example plots on the system size dependence of the ratio of K^+ and π^+ yields at mid-rapidity and of the scaled variance of multiplicity distributions. The Be+Be results are close to p+p independently of collision energy. Moreover, the data show a jump between light (p+p, Be+Be) and intermediate, heavy (Ar+Sc, Pb+Pb) systems.

Here one recalls the following:

1. The K^+/π^+ ratio in p+p interactions is below the predictions of statistical models. However, the ratio in central Pb+Pb collisions is close to statistical model predictions for large volume systems. For detail see e.g. Ref. [15]
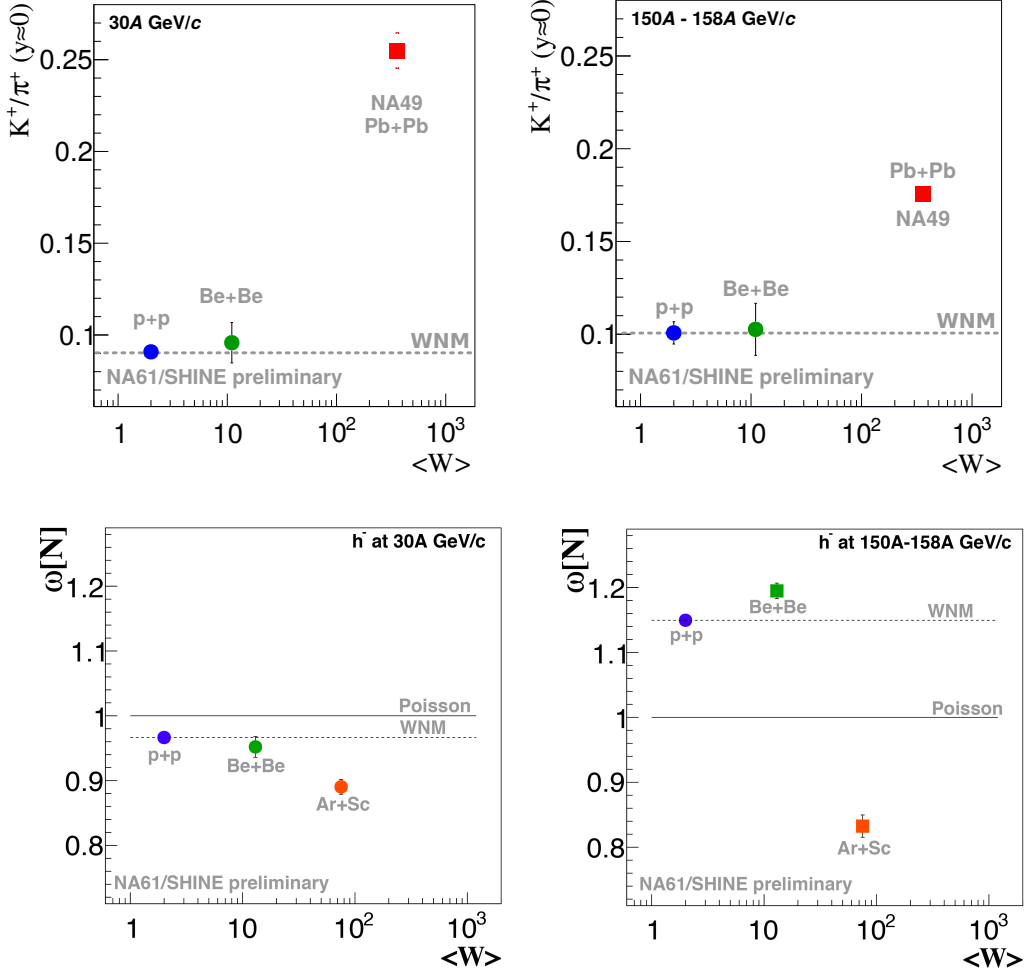
Figure 6: *Top left* and *top right*: System size dependence of the K^+/π^+ ratio at mid-rapidity at 30A GeV/c and 150A GeV/c. *Bottom left* and *bottom right*: System size dependence of the scaled variance of the multiplicity distribution of negatively charged hadrons at 30A GeV/c and 150A GeV/c.

2. In p+p interactions, and thus also in Be+Be collisions, multiplicity fluctuations are larger than predicted by statistical models. However, they are close to statistical model predictions for large volume systems in central Ar+Sc and Pb+Pb collisions, for detail see Ref. [16].

Thus the observed rapid change of hadron production properties that start when moving from Be+Be to Ar+Sc collisions can be interpreted as the beginning of creation of large clusters of strongly interacting matter - the onset of fireball [2]. We note that non-equilibrium clusters produced in p+p and Be+Be collisions seem to have similar properties at all beam momenta studied here. This is well seen in Fig. 7 where scaled variance and strongly intensive scaled variance are plotted as a function of collision energy.

Finally we recall that hadron production properties in heavy ion collisions were found to change rapidly with increasing collision energy in the low SPS energy domain, $\sqrt{s_{NN}} \approx 10$ GeV (for a recent review see Ref. [17]). The NA61/SHINE results shown in Fig. 8 indicate that this is
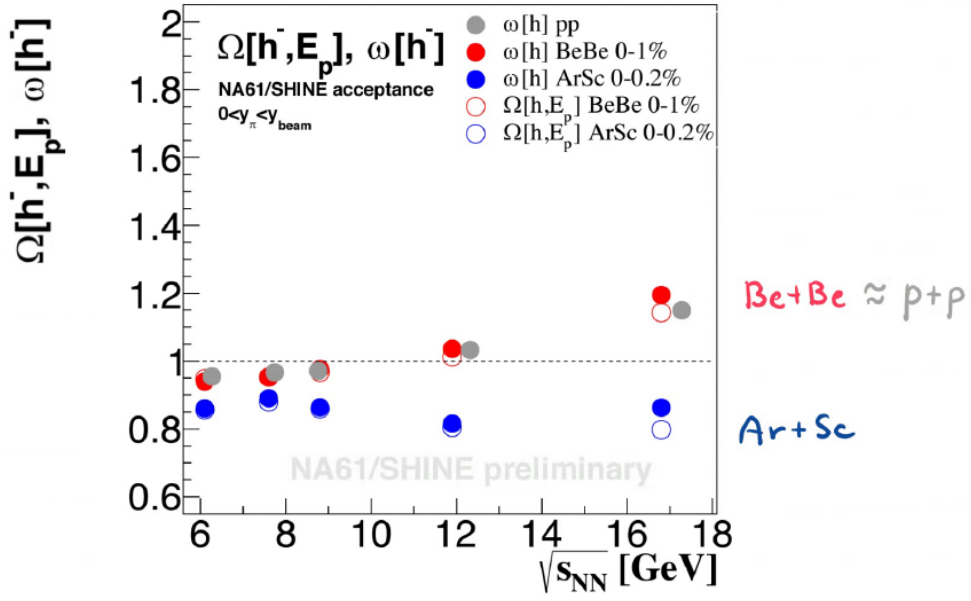
Figure 7: Collision energy dependence of scaled variance and strongly intensive scaled variance of the negatively charged hadron multiplicity distribution for inelastic p+p interactions and violent Be+Be and Ar+Sc collisions.

also the case in inelastic p+p interactions and probably also in Be+Be collisions. The phenomenon is labelled as the *onset of deconfinement* and interpreted as the beginning of creation of quark-gluon plasma with increasing collision energy [18].

Consequently the two-dimensional scan conducted by NA61/SHINE by varying collision energy and nuclear mass number of colliding nuclei indicates four domains of hadron production properties separated by two thresholds: the onset of deconfinement and the onset of fireball. The sketch presented in Fig. 9 illustrates this conclusion.
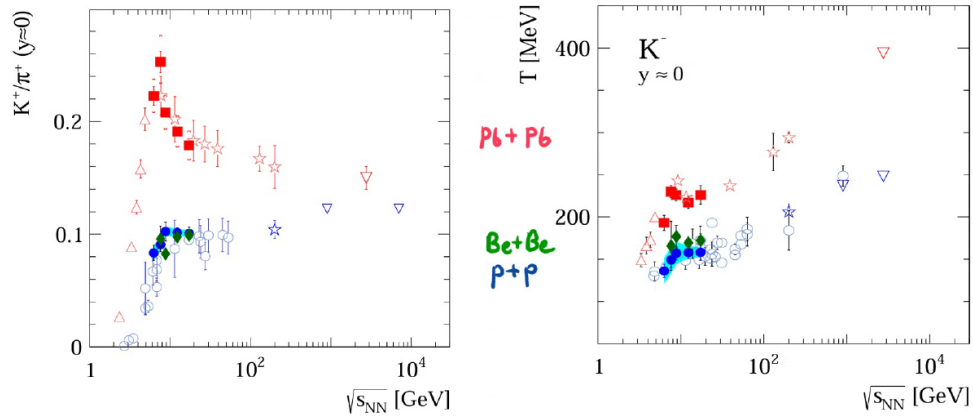
Figure 8: *Left:* Energy dependence of positively charged kaon yield divided by the corresponding charged pion yield at mid-rapidity. *Right:* Energy dependence of inverse slope parameter of transverse mass spectra of negatively charged kaons at mid-rapidity. Results for inelastic p+p interactions and violent Be+Be and Pb+Pb (Au+Au) collisions are presented.
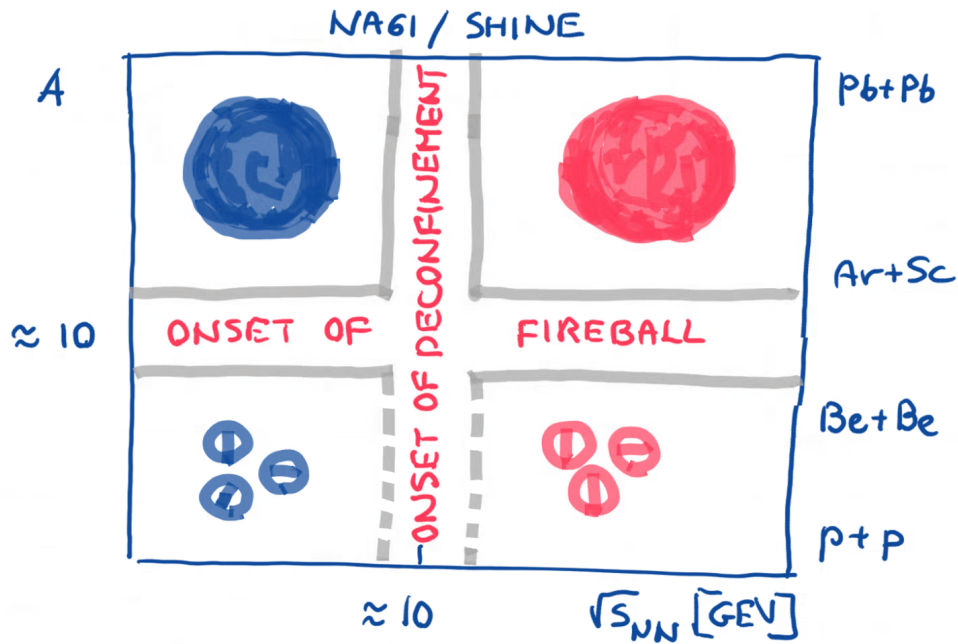

Figure 9: Two-dimensional scan conducted by NA61/SHINE by varying collision energy and nuclear mass number of colliding nuclei indicates four domains of hadron production properties separated by two thresholds: the onset of deconfinement and the onset of fireball. The onset of deconfinement is well established in central Pb+Pb(Au+Au) collisions, its presence in collisions of low mass nuclei, in particular, inelastic p+p interactions is questionable.

8

4. Search for critical point

A characteristic feature of a second order phase transition (the critical point or line) is the divergence of the correlation length. The system becomes scale invariant. This leads to large fluctuations in particle multiplicity. Moreover these fluctuations have specific characteristics [19, 20]. Also other properties of the system should be sensitive to the vicinity of the critical point [21]. Thus when scanning the phase diagram a region of increased fluctuations may signal the critical point or the critical line.

In the experimental search for the critical point one would like to minimize influence of both *volume* fluctuations and conservation laws. Thus it is recommended to use quantities which are insensitive (in the WNM and the SM(IB-GCE)) to these. It appears that strongly intensive quantities composed of suitably selected extensive quantities have this property. For example these are [7, 22]:

$$\Delta[P_T, N] = \frac{1}{\langle N \rangle \omega[p_T]}[\langle N \rangle \omega[P_T] - \langle P_T \rangle \omega[N]] \tag{4.1}$$

and

$$\Sigma[P_T, N] = \frac{1}{\langle N \rangle \omega[p_T]}[\langle N \rangle \omega[P_T] + \langle P_T \rangle \omega[N] - 2(\langle P_T N \rangle - \langle P_T \rangle \langle N \rangle)], \tag{4.2}$$

where P_T is the sum of the absolute values of transverse momenta p_T. The quantity $\omega[p_T]$ is the scaled variance of the inclusive p_T distribution (summation runs over all particles and all events)

$$\omega[p_T] = \frac{\overline{p_T^2} - \overline{p_T}^2}{\overline{p_T}}. \tag{4.3}$$

It is easy to show that $\Delta[P_T, N]$ and $\Sigma[P_T, N]$ are independent of *volume* fluctuations and material conservation laws for the SM(IB-CE).

Example results of NA61/SHINE from the search for the critical point using $\Delta[P_T, N]$ and $\Sigma[P_T, N]$ are presented in Fig. 10. No indication for the critical point is observed so far.
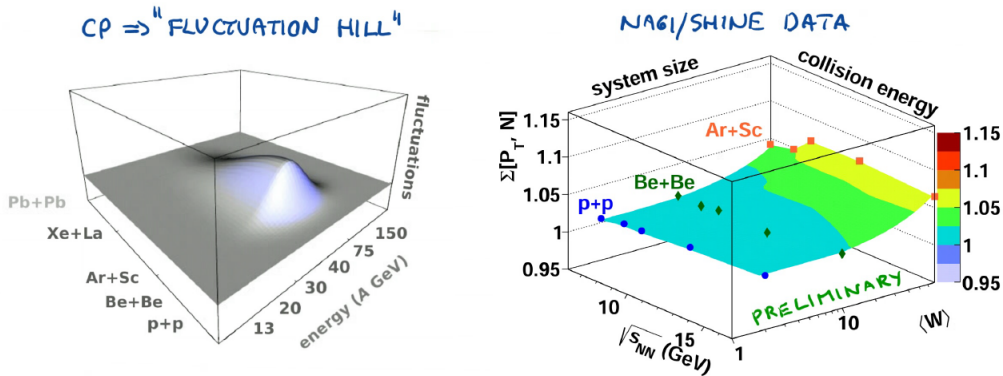

Figure 10: *Left*: Sketch of the hill of fluctuations which may be observed in the (beam momentum) - (system size) scan of NA61/SHINE provided the freeze-out parameters are close to the critical point. *Right*: $\Sigma[P_T, N]$ measured by NA61/SHINE in inelastic p+p interactions and violent Be+Be and Ar+Sc collisions at the CERN SPS energies. Results refer to negatively charged hadrons at forward rapidity ($0 < y_\pi < y_{beam}$) and $p_T < 1.5$ GeV/c.

In the grand canonical ensemble the correlation length ξ diverges at the critical point (or second order phase transition line) and the system becomes scale invariant [19, 23]. This leads to large multiplicity fluctuations with special properties. They can be conveniently exposed using scaled factorial moments $F_r(M)$ [24] of rank (order) r:

$$F_r(M) = \frac{\langle \frac{1}{M} \sum_{i=1}^{M} N_i(N_i-1)...(N_i-r+1) \rangle}{\langle \frac{1}{M} \sum_{i=1}^{M} N_i \rangle^r} \ , \tag{4.4}$$

where $M = \Delta/\delta$ is the number of the subdivision intervals of size δ of the momentum phase space region Δ. N_i refers to particle multiplicity in the interval i and $\langle ... \rangle$ indicates averaging over the analysed collisions.

In the SM(IB-GCE) one gets $F_r(M) = 1$ for all values of r and M provided the mean particle multiplicity is proportional to δ. The latter condition is trivially obeyed for a subdivision in configuration space where the particle density is uniform throughout the gas volume. For the case of subdivision in momentum space the subdivision should be performed using so-called cumulative kinematic variables [25] in which the particle density is uniform.

At the second order phase transition the matter properties strongly deviate from the ideal gas. The system is a simple fractal and $F_r(M)$ possess a power law dependence on M:

$$F_r(M) = F_r(1) \cdot M^{-\phi_r} \ . \tag{4.5}$$

Moreover the exponent (intermittency index) ϕ_r satisfies the relation:

$$\phi_r = (r-1) \cdot d_r \ , \tag{4.6}$$

with the anomalous fractal dimension d_r being independent of r [20].

Note, that $F_r(M)$ is sensitive to to both *volume* fluctuations and material conservation laws. A formulation of a new method to study intermittency using strongly intensive quantities is needed.

NA61/SHINE results and NA49 results on $F_2(M)$ for protons are presented in Fig. 11. The NA49 [26] results for violent Si+A collisions at 158A GeV are consistent with about 1% of protons obeying critical fluctuations with $\phi_2 \approx 1$. The NA61/SHINE [2] results for violent Si+A collisions at 150A GeV/c establish the upper limit for protons obeying critical fluctuations to be about 0.3%. For details see Ref. [27].
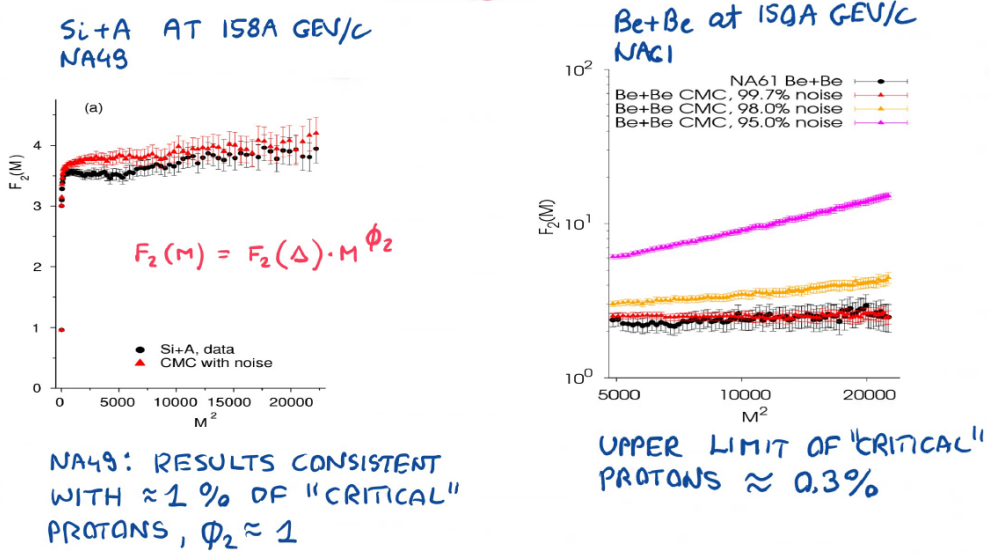
Figure 11: $F_2(M)$ of protons in violent Si+A collisions at 158A GeV/c (*left*) and in violent Be+Be collisions at 150A GeV/c (*right*). The subdivision is performed in transverse momentum plane at mid-rapidity. The results are compared to model predictions calculated for different fraction of protons obeying critical fluctuations.

11

References

[1] N. Antoniou *e*t al. [NA61/SHINE Collaboration], CERN-SPSC-2006-034.

[2] A. Aduszkiewicz *e*t al. [NA61/SHINE Collaboration], CERN-SPSC-2017-038.

[3] M. Gazdzicki and P. Seyboth, Acta Phys. Polon. B **47**, 1201 (2016).

[4] M. Gazdzicki and M. I. Gorenstein, Phys. Lett. B **640**, 155 (2006).

[5] A. Bialas, M. Bleszynski and W. Czyz, Nucl. Phys. B **111**, 461 (1976).

[6] M. Gazdzicki, Acta Phys. Polon. B **43**, 791 (2012).

[7] M. I. Gorenstein and M. Gazdzicki, Phys. Rev. C **84**, 014904 (2011).

[8] V. P. Konchakovski, S. Haussler, M. I. Gorenstein, E. L. Bratkovskaya, M. Bleicher and H. Stoecker, Phys. Rev. C **73**, 034902 (2006).

[9] M. Gazdzicki and S. Mrowczynski, Z. Phys. C **54**, 127 (1992).

[10] E. Sangaline, arXiv:1505.00261 [nucl-th].

[11] A. Seryakov *et al.* [NA61/SHINE Collaboration], talk at CPOD 2017.

[12] W. Florkowski, "Phenomenology of Ultra-Relativistic Heavy-Ion Collisions, Singapore: World Scientific (2010) 416 pages.

[13] J. Rafelski and M. Danos, Phys. Lett. **97B**, 279 (1980).

[14] V. V. Begun, M. Gazdzicki, M. I. Gorenstein and O. S. Zozulya, Phys. Rev. C **70**, 034901 (2004).

[15] F. Becattini, J. Manninen and M. Gazdzicki, Phys. Rev. C **73**, 044905 (2006).

[16] V. V. Begun, M. Gazdzicki, M. I. Gorenstein, M. Hauer, V. P. Konchakovski and B. Lungwitz, Phys. Rev. C **76**, 024902 (2007).

[17] M. Gazdzicki, M. I. Gorenstein and P. Seyboth, Int. J. Mod. Phys. E **23**, 1430008 (2014).

[18] M. Gazdzicki, M. Gorenstein and P. Seyboth, Acta Phys. Polon. B **42**, 307 (2011).

[19] J. Wosiek, Acta Phys. Polon. B **19**, 863 (1988).

[20] A. Bialas and R. C. Hwa, Phys. Lett. B **253** (1991) 436.

[21] M. A. Stephanov, K. Rajagopal and E. V. Shuryak, Phys. Rev. D **60**, 114028 (1999).

[22] M. Gazdzicki, M. I. Gorenstein and M. Mackowiak-Pawlowska, Phys. Rev. C **88**, no. 2, 024907 (2013).

[23] H. Satz, Nucl. Phys. B **326**, 613 (1989).

[24] A. Bialas and R. B. Peschanski, Nucl. Phys. B **273**, 703 (1986).

[25] A. Bialas and M. Gazdzicki, Phys. Lett. B **252**, 483 (1990).

[26] T. Anticic *et al.* [NA49 Collaboration], Eur. Phys. J. C **75** (2015) no.12, 587.

[27] N. Davis *et al.* [NA61/SHINE Collaboration], talk at CPOD 2017.